

On Solving Quantum Walker Using Steepest Entropy Ascent Ansatz

Rohit Kishan Ray

E-mail: rohitkray@iitkgp.ac.in

Department of Physics, Indian Institute of Technology Kharagpur, India - 721302

Abstract. We use steepest entropy ascent (SEA) ansatz on single and double quantum walker (QWer). We arrive both at typicality proposed by eigenstate thermalization hypothesis (ETH), and many body localization (MBL) states under varied conditions. Showing analytically and graphically, one can use SEA induced dynamics to reach ETH/MBL states in order to study open quantum systems.

PACS numbers:

1. Introduction

Physicists have been taking multiple attempts towards understanding open quantum systems [1]. Of the major pathways, eigenstate thermalization hypothesis (ETH) and subsequently typicality has gained significant attention [2, 3, 4, 5, 6, 7, 8, 9, 10, 11, 12, 13, 14, 15]. The emergence of typicality in a quantum system has been discussed in a recent review by [11]. Our present work is based on this review. As discussed by Goldstein *et al.* [4], the statement of typicality can be understood as follows: *in the thermodynamic limit, the reduced density matrices of the overwhelming majority of the wave-functions of a micro-canonical ensemble are canonical.* A kinematic study of the same is discussed by [3], whereas the role of typicality in Random Matrix Product states has been highlighted by [5]. For the many body cases, weak and strong typicality have been shown by [6]. We see that the theoretical formalism falls short in explaining the concept of eigenstate thermalization and many-body localization under the same structure [11]. Although there have been considerable efforts towards the development of a coherent quantum theory (for instance, see [16, 17, 18]); yet, the problem remains open. In their recent work, [7] raise the concern over the time-scale on which pre-thermalization occurs, which is a behaviour similar to achieving a quasi-equilibrium state before thermalization happens. The problem of time scales and conditions of equilibrium in this context is also raised in the work by [8] as well.

Getting back to the case of open quantum systems, we find another pathway leading towards a bold and different idea: what if the system in discussion is moving spontaneously towards a stable orbit by invoking the second law of thermodynamics as a fourth postulate of quantum mechanics [19, 20, 21, 22, 23, 24]? This idea has led us to the steepest entropy ascent (SEA) ansatz. In the language stated in [25], the SEA problem is *to solve the variational problem by finding the instantaneous “direction” of rate of change of state function by maximizing entropy production rate subject to certain constraints.* After remaining dormant for a couple of decades, this theory was independently brought to surface by [26] and since then it has gained appreciable support. SEA has shown promise in explaining the origin of non-linearity in quantum mechanics [27, 28], provided a geometric framework for understanding the principle of maximum entropy generation [25] and has been exploited in-order to understand electron and phonon transport [29, 30]. Besides, it has been compared to *general equation for the nonequilibrium reversible-irreversible coupling (GENERIC)* theory, and has been found to be on par with it [31].

The above mentioned approaches differ from each other despite attempting to address the same problem of open quantum systems. SEA stresses on the drive for stability to the canonical quantum mechanics, whereas ETH/MBL describe entropy as an emergent phenomena. The distinct characteristics of SEA is that it can be applied to one or many particle systems, as we will see in this paper. Moreover, when we apply SEA on a quantum walker on a graph of uniform ring, we get both unitary and non-unitary behaviours under certain conditions. On increasing the number of particles

to two, we start observing distinct changes in the evolution of entropy functional over time. We see that this change depends mainly on the amount of perturbation the initial state goes through, and on the relaxation time of the system. Thus, we get our first hint for typicality. Secondly, we do show at certain conditions we are getting canonical like behaviour in the probability distribution which also concurs with the statement of typicality. Thus, SEA has been directing about a coherent pathway towards the problem raised by [11]. Although typicality finds a small mention in the work of [32], to the best of our knowledge, there hardly has been any attempt in taking this route towards resolving ETH and MBL dichotomy. Our analytical and numerical results shows agreement between SEA evolved result and typicality condition.

Before we move on with our discussion, we feel the need to justify the choice of quantum walk (QW) as our model. QW has played a pivotal role in searching algorithms [33, 34], and in quantum computation [35]; primarily because of its unique ballistic nature and speed [36] compared to that of classical random walk. Many body walks have been is one of the suitable approaches to understand the nature of entanglement in multipartite systems [37, 38, 39, 40, 41]. There has also been a substantial amount of work in understanding dissipative quantum walks [42, 43, 44, 45]. So we stand a clear ground on the applicability of QW as a test model for SEA formalism. Moreover, experiments have been performed involving QW [46, 47, 48, 49], and the theoretical results stand on firm grounds (for a detailed review on QW, see [50] and references therein). In literature, there are mainly two types of QW, continuous time and discrete time, also known as CTQW and DTQW respectively. We have chosen CTQW for our modelling as it does not require a coin operator [51]. So we can incorporate the transition matrix between modes as a Hamiltonian governing the system [51]. Another reason for avoiding coin operator in our study was also to exclude multiple coins and interactions due to it [43, 52].

QW is unitary by nature, hence reversible; SEA formalism has been used to comprehend properties of the system under consideration by studying unitary evolution [53]. Inspired by this approach, we have studied a slightly perturbed single and double walker state evolve under SEA considerations and reach the approximate unitary nature. In doing so, we have identified certain components that may help us in exploring different regimes in CTQW. We have witnessed the emergence of typicality like behaviour in single and double particle states. We have also identified possibilities of high negative entropic states closer to the thermodynamic equilibrium state, and a relative time scale in which this observation can be made. In our search for signs of typicality, we have also ended up showing that SEA framework is suitable for studying the emergence of typicality in quantum systems, and has a much greater range of applications left for exploration. To the best of our knowledge, this paper addresses a novel link bridging the framework of SEA and that of ETH/MBL, that is, quantum walk.

We present this paper in the following order: in section 2, we will provide a short overview of the theory available in the literature regarding SEA and QW. In the latter part of this section, we have taken the specific case of walker(s) walking on a ring of

N nodes. We have provided the solution to the dynamical equation of motion in the section 3 titled Results. A detailed discussion on the solution is provided in appendices cited herein. In the latter part of this section, we present the numerically plotted results followed by a discussion on them. We also have attempted to provide physical reasoning for the results that we have obtained. We present our conclusion the section 4 with a summary of the work presented in this study with questions, possible answers and more probable questions. Finally, we conclude by acknowledging valuable contributions towards our work in the section 5.

2. Theoretical Background

The main contribution of SEA in the domain of open quantum mechanics is the introduction of a fourth postulate in addition to existing postulates of quantum mechanics. Let us revisit the postulates for the sake of continuity [19, 54].

- 1: *Correspondence Postulate*: Any isolated physical system can be associated with a complex vector space with inner products (Hilbert space), we call it *state space* ($|\psi\rangle$) of the system. The system is completely described by its associated state vector.
- 2: *Dynamical Postulate*:
 - (a) Any two states of a system that are interconnected by a physical process can always be interconnected by means of one or more reversible processes.
 - (b) For every system, reversible separable processes always exist for which the temporal development of the density operator $\hat{\rho}$ is given by the relation:

$$\hat{\rho}(t_2) = \hat{U}(t_2, t_1)\hat{\rho}(t_1)\hat{U}^\dagger(t_2, t_1), \quad (1)$$

where $\hat{U}(t_2, t_1)$ is a unitary operator in time (evolution operator), and $\hat{U}^\dagger(t_2, t_1)$ is the Hermitian conjugate of $\hat{U}(t_2, t_1)$.

- 3: *Measurement Postulate*: Quantum measurements are described by the expectation values of Hermitian real operators M_m acting on the state space. The outcomes span the eigenspace of the measurement operator, and also satisfy the completeness condition. Post measurement, the state of the system is $M_m |\psi\rangle$ with proper normalization.
- 4: *Stable-Equilibrium Postulate*: Any independent separable system subject to fixed parameters has a unique stable equilibrium state for each set of (expectation) values of energy and numbers of particles of constituent species.

The fourth postulate as presented above is the root of amalgamation of thermodynamics with quantum mechanics. Stability as discussed in the above statement is to be followed in Lyapunov sense[‡][28]. But Lyapunov stability is about local stability and the second

[‡] A state ρ_e is an *equilibrium* state iff the generator of trajectories follow $u(t, \rho_e) = \rho_e$ for all times t . An equilibrium state ρ_e is *locally stable* iff $\forall \epsilon > 0, \exists \delta(\epsilon) |d(\rho, \rho_e) < \delta(\epsilon) \implies d(u(t, \rho), \rho_e) < \epsilon, \forall t > 0, \wedge \forall \rho$. A system is *unstable* iff it is not locally stable.

law of Thermodynamics demands for a global stability, which is a weaker condition as it also includes metastability§. The concept of global stability as drawn from the second law can be stated as follows.

An equilibrium state is *globally stable* if for every $\eta > 0$ and every $\epsilon > 0$ there exists a $\delta(\epsilon, \eta) > 0$ such that every trajectory $u(t, \rho)$ with $\eta < d(u(t, \rho), \rho_e) < \eta + \delta(\epsilon, \eta)$, i.e., passing at time $t = 0$ between distance η and $\eta + \delta$ from ρ_e , remains within $d(u(t, \rho), \rho_e) < \eta + \epsilon$ for every $t > 0$, proceeds in time without ever exceeding the distance $\eta + \epsilon$ [55] ($d(\rho_1, \rho_2)$ is a measure of distance between two states ρ_1 and ρ_2).

As demanded by the second law of thermodynamics, a system spontaneously moves towards the global equilibrium. We can consider that the states for which $\rho^2 = \rho$ ('pure' Quantum Mechanics, or unitary dynamics), are globally stable, and every other system is trying to achieve that Thermodynamic equilibrium with its environment. The steepest-entropy-ascent (SEA) formalism traces out a path in the ρ space which maximizes entropy generation and guides the system towards the thermodynamic equilibrium.

The notation and terminology presented in this work are followed from reference [25] including some of the basic equations that we consider as our starting point. Below, we revisit those equations for the ease of the reader and the coherence of this paper.

In the SEA formalism, in order to maintain the preservation of non-negativity and the self-adjointness of density operator (ρ) during its evolution through time [25] the positive square-root of ρ is used to represent the state. We denote it by γ , and use spectral theorem [27] to compute them. We can reconstruct ρ using the following equation:

$$\rho = \gamma\gamma^\dagger. \quad (2)$$

We consider a state space (\mathcal{L}), a manifold in a Hilbert space equipped with an inner product ($\cdot | \cdot$). We denote its elements (the states) by γ or alternatively $|\gamma\rangle$. For SEA, the inner product is defined as:

$$(A | B) = \text{Tr}(A^\dagger B + B^\dagger A)/2. \quad (3)$$

Real functionals $\tilde{A}(\gamma), \tilde{B}(\gamma), \dots$ of γ represent system properties, i.e., energy, entropy, mass, momentum, etc.; such that their functional derivatives with respect to γ are also elements of \mathcal{L} ; we denote them by $\delta\tilde{A}(\gamma)/\delta\gamma$ or, alternatively, by $|\delta\tilde{A}(\gamma)/\delta\gamma\rangle$. Under the SEA criteria, we find the equation of motion to be of the form (see Appendix A for the derivation):

$$\frac{d\rho}{dt} = -2\hat{L} [k[\ln(\rho), \rho]_+ + \beta_H[\mathbf{H}, \rho]_+ + \beta_I[\mathbf{I}, \rho]_+] - \frac{i}{\hbar}[\mathbf{H}, \rho]_-. \quad (4)$$

§ An equilibrium state is *metastable* iff it is locally stable but $\exists \eta > 0 \wedge \epsilon > 0 | \forall \delta > 0, \exists u(t, \rho)$ with $t > 0$ at a distance farther than $\eta + \epsilon, d(u(t, \rho), \rho_e) \geq \eta + \epsilon$.

We have \mathbf{H} as the system Hamiltonian, \mathbf{I} as an identity operator to preserve probability, β_H , and β_I are the corresponding Lagrange multipliers respectively. k is Boltzmann constant, $\hat{L} = \frac{1}{\tau}\hat{G}(\gamma)^{-1}$ (A.11), where, \hat{G} is the metric associated with the ρ space, and τ is another Lagrange multiplier. The above equation has the following general structure:

$$\frac{d\rho}{dt} = -[\mathcal{D}, \rho]_+ - i[\mathbf{H}, \rho]_- \quad (5)$$

The anti-commutator part represents dissipation and the commutator part represents evolution. Prompting to see the evolution in two parts. Similar kind of dissipative operators \mathcal{D} (albeit with different internal structure [31]) exists in other open quantum theories as well. We see a competition between \mathcal{D} and \mathbf{H} as soon as we disturb the system from one of its stable equilibriums. Just like the operator \mathbf{H} , the dissipative operator \mathcal{D} is not responsible for the changes in the invariant functionals i.e., \tilde{C}_i [56]. Thus a pure state has unitary evolution under \mathbf{H} , and a thermodynamic stable state remains so. To see the effect of SEA, we need to slightly disturb the initial pure state and then apply variational principle (experimentally this can be done by *quenches*, see [12]) [29]. We have,

$$\rho_{\text{SEA},0} = \epsilon\rho_0 + (1 - \epsilon)\rho_{\text{therm}} \quad (6)$$

Where, ϵ is a perturbation parameter ($\epsilon \in [0, 1]$). For our numerical computation ϵ has range $(0, 1]$. Here, ρ_{therm} is the thermodynamic equilibrium state, and $\rho_{\text{SEA},0}$ is the initial state for SEA evolution. For the walker(s), we have considered the following two cases:

- (i) *Micro canonical*: In this case, we have considered the walker and the graph to be isolated from all other interactions. Under this criteria, equation (6) becomes:

$$\rho_{\text{SEA},0} = \epsilon\rho_0 + (1 - \epsilon)\frac{\mathbf{I}_N}{\text{Tr}\{\mathbf{I}_N\}} \quad (7)$$

where \mathbf{I}_N is the identity matrix of order N .

- (ii) *Canonical*: Here, the canonical probability distribution is given as [11, 53] $\rho_{\text{can}} = \frac{\exp(-\beta\mathbf{H})}{\text{Tr}\{\exp(-\beta\mathbf{H})\}}$, and thus, equation (6) becomes,

$$\rho_{\text{SEA},0} = \epsilon\rho_0 + (1 - \epsilon)\rho_{\text{can}} \quad (8)$$

We will apply the concept of SEA onto CTQW. One of the efficient ways to compute quantum walk is to consider the graph theoretical approach as followed by most physicists in literature [50]. We consider a graph \mathcal{G} of a ring with N number of nodes, where N^{th} node is connected to 1^{st} node via an edge. The Laplacian [57, 33] can be written as follows:

$$\mathbf{L} = \mathbf{A} - \mathbf{D}, \quad (9)$$

where \mathbf{A} and \mathbf{D} (adjacency and degree matrix respectively), are associated with the graph \mathcal{G} . The Laplacian acts as a node to node transition matrix. Thus, we are not worried about the discretization of time, rather are interested in the probability

amplitude corresponding to each such transition. Each step is an integer number to correspond to each level of transition irrespective of time taken to make that transition. In the standard basis, we can represent the Laplacian for \mathcal{G} as,

$$\mathbf{L} = \begin{bmatrix} -2 & 1 & 0 & \dots & 1 \\ 1 & -2 & 1 & 0 & \cdot & \cdot & 0 \\ 0 & 1 & -2 & 1 & \cdot & \cdot & \cdot \\ \vdots & & & \ddots & & & \vdots \\ 1 & 0 & \dots & & 1 & -2 \end{bmatrix}. \quad (10)$$

The Hamiltonian of the continuous time random walk can be written as [51],

$$\mathbf{H} = -\mu\mathbf{L}, \quad (11)$$

where, μ is the transition rate from one mode to another, here considered to be uniform for all possible transitions. Using this Hamiltonian, the unitary evolution of the walker can be written in the form ($\hbar = 1$),

$$\rho(t_2) = \exp(i\mu\mathbf{L}(t_2 - t_1))\rho(t_1) \exp(-i\mu\mathbf{L}(t_2 - t_1)). \quad (12)$$

For both one and two particle cases, we have considered \mathbf{H} to be the SEA Hamiltonian as well. SEA provides us a general picture of evolution under a given \mathbf{H} , and we can verify the results by arriving at quantum mechanical results under appropriate limits. Following the SEA formalism as described above and utilizing equations (2),(A.1)-(A.6), & (A.10) we get,

$$\rho_{\text{SEA},0} = \gamma_0\gamma_0^\dagger. \quad (13)$$

The quantities β_i given in equation (A.10) can be solved using the identities of equations (A.2), & (A.3) (see Appendix B) and thus we get the equation of motion in terms of γ as:

$$\frac{d\gamma}{dt} = \hat{L} [-2k \ln(\gamma\gamma^\dagger)\gamma - 2\beta_H\mathbf{H}\gamma - 2\beta_I\gamma] \quad (14)$$

The solution to the above equation in terms of ρ_{SEA} is given as (see Appendix C for detailed solution):

$$\rho_{\text{SEA},t} = e^{-i\mathbf{H}(t)}\mathbf{S}e^{\mathcal{D}(t)}(e^{\mathcal{D}(t)})^\dagger\mathbf{S}^{-1}e^{i\mathbf{H}(t)} \quad (15)$$

where,

$$\mathcal{D}(t) = \frac{A_0 \exp\left(\exp(-4k\hat{L}t) - 1\right) - \beta_H\mathbf{S}^{-1}\mathbf{H}\mathbf{S} - \beta_I}{2k}, \quad (16)$$

and, A_0 is given by

$$A_0 = k \ln\left(\gamma_{D,0}\gamma_{D,0}^\dagger\right) + \beta_H\mathbf{S}^{-1}\mathbf{H}\mathbf{S} + \beta_I \quad (17)$$

Equation (15) displays the competition between \mathcal{D} and \mathbf{H} as discussed above. The iterative solution can be updated to get $\rho_{\text{SEA},t}$, where, the initial state is the perturbed state as given in equations (7) and (8).

3. Results

The main objective of this work is to establish a link between Typicality/ETH and MBL via SEA. To achieve that, we have considered CTQW for a single walker and for double walker. The density matrices to initiate the processes have been chosen in the following way.

(i) Single walker: $\rho_0 = |i\rangle \langle i|$

(ii) Double walker:

Non interacting: $\rho_0 = \rho_1 \otimes \rho_2$

Fermionic interaction: $\rho_0 = (|i, j\rangle - |j, i\rangle)(\langle i, j| - \langle j, i|)/2$

Bosonic interaction: $\rho_0 = (|i, j\rangle + |j, i\rangle)(\langle i, j| + \langle j, i|)/2$

Also, the two particle Hamiltonian is taken in the form $\mathbf{H} = \mathbf{H}_1 \otimes \mathbf{I} + \mathbf{I} \otimes \mathbf{H}_2$. Our results will be presented in two parts, first part consisting of the analysis of probability and the second part will consist of the same on entropy.

The CTQW model that we have has $N = 100$ nodes for single walker and $N = 30$ nodes for double walker^{||} and it has been solved using SEA. One of the tests of SEA is that for $\epsilon \rightarrow 1$ limit, it should return quantum mechanical values. And, for lower ϵ values we should be getting thermodynamic stable states. To verify this, we first present the plot of the unitary quantum walk. We have simulated the walk on the basis of some assumptions, (i) the value of μ is taken to be one [50]. (ii) The metric \hat{G} has been considered to be of Euclidean type [32], that is identity matrix. The walker distribution is generated over 10 steps to give an idea of the unitary evolution as shown in Fig. 1 below. Next, we will show the simulation resulted from using the solution as found in equation (15) in the two different regimes as discussed above.

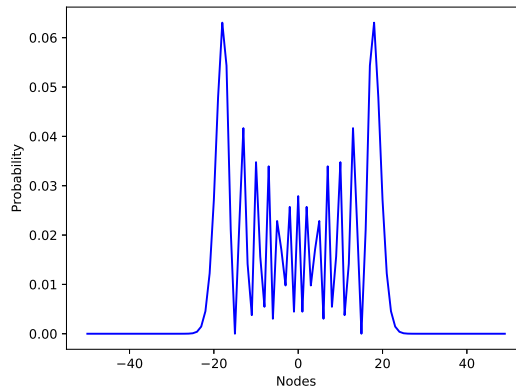


Figure 1. (Colour online) Probability distribution for a single quantum walker on a ring of 100 nodes. The walker was initiated at node 50, and the probability distribution is for after 10 steps. In this diagram, node 50 is shifted to node 0.

^{||} As the tensor product space starts increasing, higher N value requires much more computation time.

3.1. Probability

In this section we will discuss the probability distributions that we have found and compare those results to the unitary behaviour as noted in Fig. 1. We will be plotting both single particle and double particle (reduced density matrix plot) to compare the cases under the domains of micro-canonical and canonical conditions.

3.1.1. Micro-canonical: In this case, the initial density matrix for SEA formalism is given by equation (7). Allowing ϵ to take the limits in the theoretical interval $[0, 1]$, we find the limiting forms of the probability distributions. From the Fig. 2, we see the

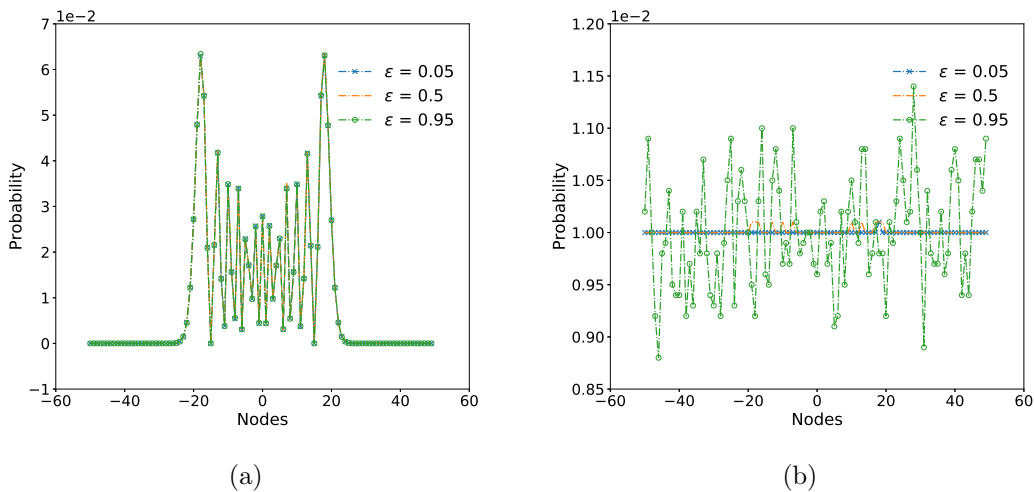


Figure 2. (Colour online) Probability distribution for a single quantum walker on a ring of 100 nodes under SEA conditions, initiated at node 50 (shifted to node 0 for symmetry), after 10 steps. The relaxation time τ is taken to be (a) 90.02 and (b) 0.02 respectively. ϵ is the dimensionless parameter denoting the perturbation of the initial state. The terms $1e-2$ appearing on the top left corner of the plots denote the order of magnitude of probability values, which in this case is 10^{-2} .

results of SEA agreeing to quantum mechanical results (Fig. 1) under the limit $\epsilon \rightarrow 1$ and high τ . We also find similar behaviour for the double particle case as well as seen in the figure. What is interesting to find is the behaviour of the system in the low τ region. The fluctuating probability denotes a well spread-out behaviour which is reminiscent of thermodynamic stable state and is not shown by CTQW. The spread of the walk under SEA also catches up to the quantum walk ballistic spread that it is known for. As we can see from Fig. 2(b), the spread increases in the low τ region. It is intriguing to notice a distinction in the probability distributions. The effect of τ is much stronger than the influence of ϵ . As seen in the panel 2(a), even for almost zero ϵ , because of high τ we could recover unitary dynamics. In fact, for sufficiently high τ , thermalization doesn't happen at all.

When looked across the panels of Fig. 3, we see that bosonic and non-interacting case has similar evolution, although with different magnitudes. The interesting case

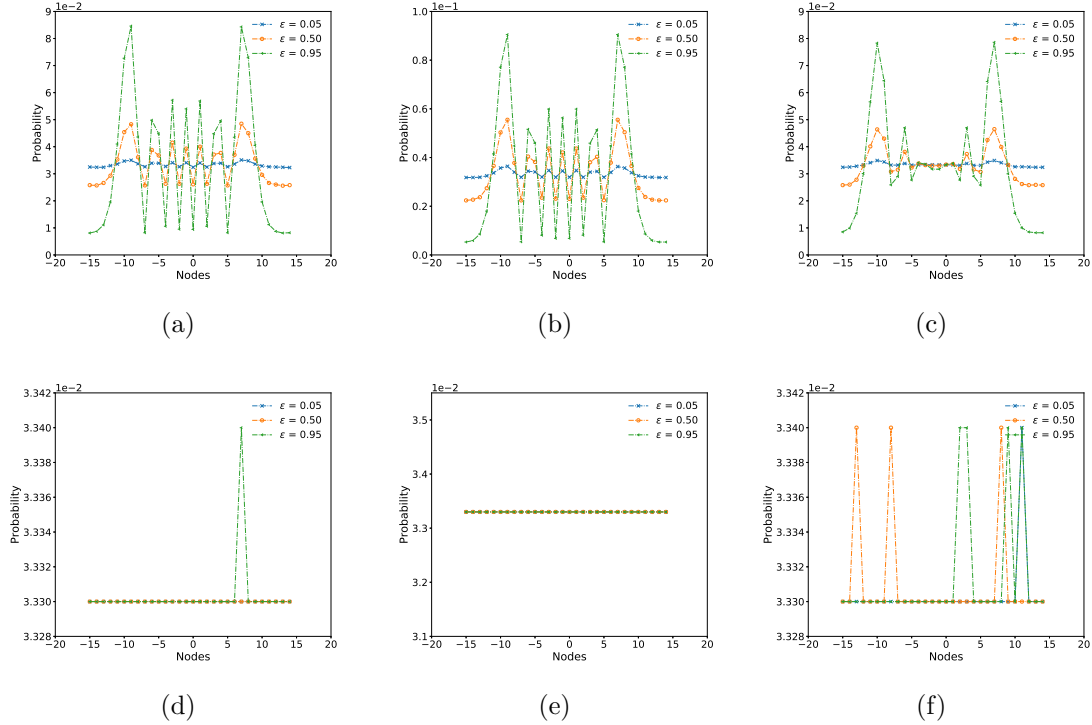


Figure 3. (Colour online) Reduced probability distribution for a double particle quantum walk on a ring of 30 nodes under SEA conditions, initiated at node 15 (shifted to node 0 for symmetry), after 5 steps. The relaxation time τ is taken to be 90.02 (in (a) to (c)) and 0.02 (in (d) to (f)) respectively. ϵ is the dimensionless parameter denoting the perturbation of the initial state. The terms $1e - 2$ appearing on the top left corner of the plots denote the order of magnitude of probability values, which in this case is 10^{-2} . The reduced probability distribution is achieved by performing partial trace on the double walker $\rho_{SEA,t}$. Panels (a) and (d) for the non-interacting cases, (b) and (e) for bosonic cases, and the last two are for the fermionic cases as discussed in the text.

arises to be the fermionic walker, that has the maximum ballistic features in the five steps that has been taken into consideration. In the bottom panels, we see statistically insignificant fluctuations and that's mostly it.

3.1.2. Canonical: We are considering the walker to be in contact with a thermal bath, and the walker and the bath compose an isolated system. We have also considered the eigenstates of the bath to be the eigenstates of the Hamiltonian associated with the graph \mathcal{G} as considered in section (2). β represents the inverse temperature associated with the bath. We have considered two ranges of β , one of the order of 10^{-1} , and another of the order of 10^{16} in natural units as discussed below to plot the probability distribution. Describing the temperature of a single walker is not something that is well understood in the literature. So, we have tried to stay away from defining it at this point. It would be much safer to say β is a parameter with temperature ‘like’ properties.

Besides, finite level systems on solving for partition function at a finite energy, result

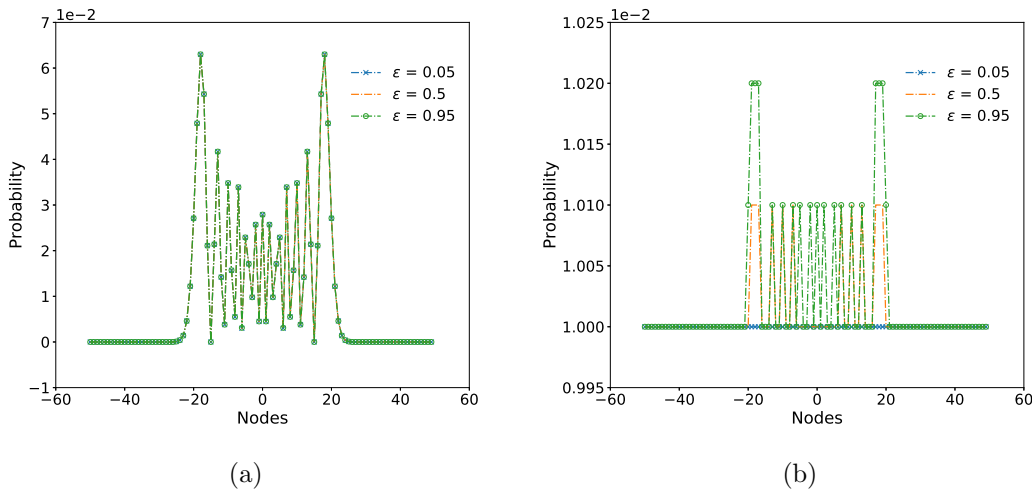


Figure 4. (Colour online) Probability distribution for a single quantum walker on a ring of 100 nodes under SEA conditions. The walker was initiated at node 50, and it is taken after 10 steps. The relaxation time τ is taken to be (a) 90.02 and (b) 0.02 respectively, whereas, ϵ is the dimensionless parameter denoting the perturbation of the initial state. The β of the heat-bath is considered to be 0.022 nats.

in negative temperature solutions. Yet, to have some context, we will be considering temperature in the information theoretic sense, and consider natural units for expressing the same. Here, we take β as calculated in the eigenspace of Hamiltonian as follows ($\ln(2)/\beta$ is the amount of energy required to erase one qubit of information in $k_B = 1$ units (see [58] for experiments on this), here we have considered average temperature available to each eigenvalue),

$$\beta = \frac{2\pi \ln(2)}{\text{Tr}(E)}, \quad (18)$$

where, E is the diagonalized form of \mathbf{H} and $k_B = 1$. For our particular example, $\beta = 0.022$ and 0.022×10^{18} in natural units for single particle, and $\beta = 0.012$ and 0.012×10^{18} for double particle. Firstly, we plot the thermal evolution plots similar to the figure (2(a)). In the first panel of the figure (4), we see a behaviour almost similar to that of the figure (2(a)). The second panel of the figure (4) deviates from that of the figure (2(b)) in the sense that despite low values of τ preserving thermal behaviour, in case of low β , the ballistic nature of the walk is retained over the spectrum of ϵ values (figure (4(b))). In case of high τ as well as high β , we can expect to see heavy dependence on ϵ as seen in figure (5(a)).

Considering similar scenarios for the double walker case, we see a distinction emerge between the low τ behaviours of the same (Fig. 6(d)-6(f)) when compared with the same in micro-canonical regime (Fig. 3(d)-3(f)). Despite it still remaining characterless as before, there's much more fluctuation this time. Besides this behaviour, the other properties remain more or less the same.

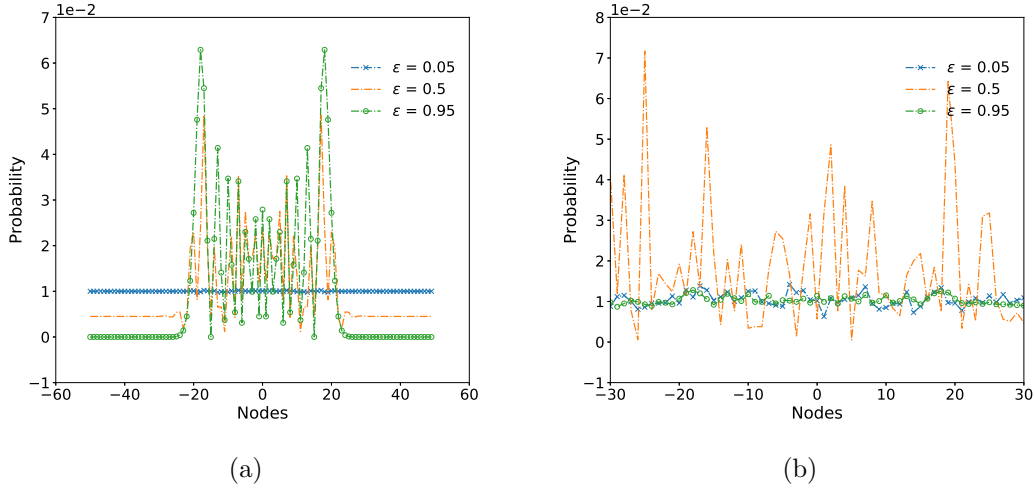


Figure 5. (Colour online) Probability distribution for a single quantum walker on a ring of 100 nodes under SEA conditions. The walker was initiated at node 50, and it is taken after 10 steps. The relaxation time τ is taken to be (a) 90.02 and (b) 0.02 respectively, whereas, ϵ is the dimensionless parameter denoting the perturbation of the initial state. The β of the heat-bath is considered to be 0.022×10^{18} nats.

3.2. Entropy

The application of SEA on CTQW presents us with the following domains **Table 1**. Here, we present the behaviour of the entropy functional \tilde{S} and its growth rate Π_S in

$\tilde{S}_{\tau\epsilon}, \Pi_{S,\tau\epsilon}$	$\epsilon \rightarrow 0$	$\epsilon \rightarrow 1$
$\tau \rightarrow 0$	$\tilde{S}_{00}, \Pi_{S,00}$	$\tilde{S}_{01}, \Pi_{S,01}$
$\tau \rightarrow \infty$	$\tilde{S}_{\infty 0}, \Pi_{S,\infty 0}$	$\tilde{S}_{\infty 1}, \Pi_{S,\infty 1}$

Table 1. Limits for entropy analysis of SEA assisted CTQW. $\lim_{\tau, \epsilon \rightarrow} \tilde{S}$ and $\lim_{\tau, \epsilon \rightarrow} \Pi_S$ are represented by $\tilde{S}_{\tau\epsilon}$, and $\Pi_{S,\tau\epsilon}$ respectively.

the SEA assisted CTQW as they appear in Table. 1. Starting with the expression $\tilde{S} = -k \text{Tr}(\gamma \ln(\gamma \gamma^\dagger) \gamma^\dagger)$, we seek out the limits of $\tau \rightarrow 0$ and some large limit $\tau \rightarrow \infty$. We have distributed the limit over the products as the individual limits exist (see derivation in [Appendix D](#)).

$$\begin{aligned}
\lim_{\tau \rightarrow 0} \tilde{S} &= \mathbf{S} \lim_{\tau \rightarrow 0} \tilde{S}_D \mathbf{S}^{-1} \\
&= -2k \text{Tr} \left[\mathbf{S} \left(\lim_{\tau \rightarrow 0} \exp(\mathcal{D}) \right) \mathbf{S}^{-1} \mathbf{S} \left(\lim_{\tau \rightarrow 0} \mathcal{D} \right) \mathbf{S}^{-1} \mathbf{S} \left(\lim_{\tau \rightarrow 0} \exp(\mathcal{D}) \right) \mathbf{S}^{-1} \right], \\
&= -\frac{1}{e} \text{Tr} \left[(\rho_{\text{SEA},0})^{1/e} \mathbf{S} \exp \left(\frac{1-e}{ke} (\beta_H \mathbf{S}^{-1} \mathbf{H} \mathbf{S} + \beta_I) \right) \mathbf{S}^{-1} (\ln(\rho_{\text{SEA},0}) + (1-e)k(\beta_H \mathbf{H} + \beta_I)) \right].
\end{aligned} \tag{19}$$

And:

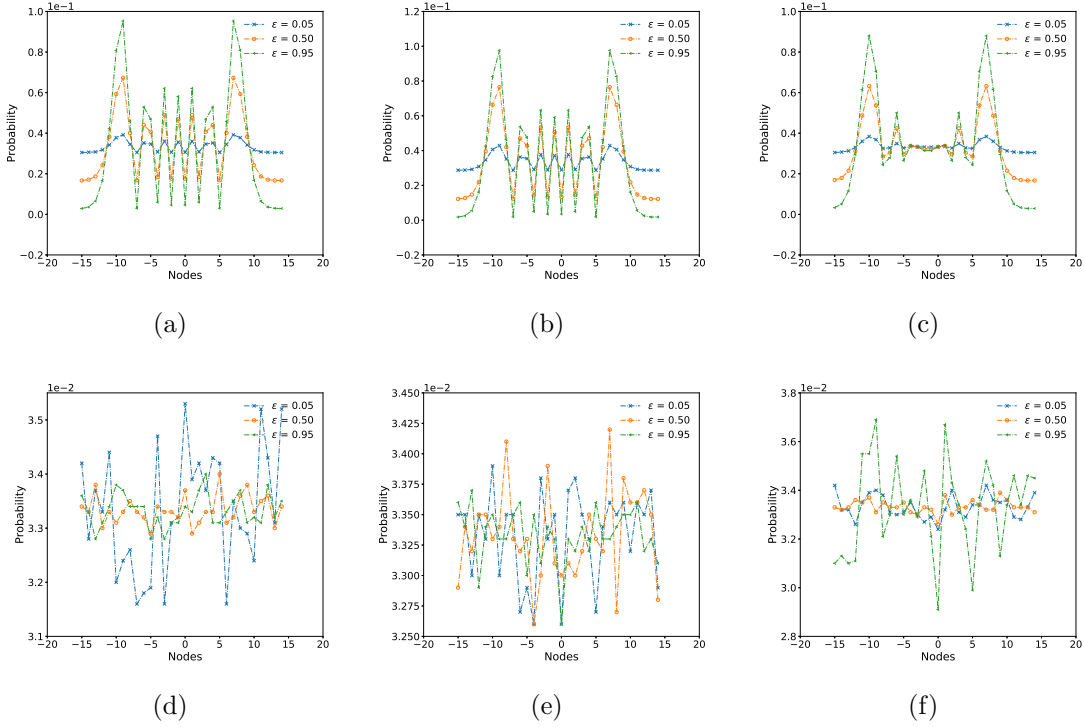


Figure 6. (Colour online) Reduced probability distribution for a double particle quantum walk on a ring of 30 nodes under SEA conditions, initiated at node 15 (shifted to node 0 for symmetry), after 5 steps. The relaxation time τ is taken to be 90.02 (in (a) to (c)) and 0.02 (in (d) to (f)) respectively. ϵ is the dimensionless parameter denoting the perturbation of the initial state. The terms $1e-2$ appearing on the top left corner of the plots denote the order of magnitude of probability values, which in this case is 10^{-2} and 10^{-1} . The reduced probability distribution is achieved by performing partial trace on the double walker $\rho_{SEA,t}$. Panels (a) and (d) for the non-interacting cases, (b) and (e) for bosonic cases, and the last two are for the fermionic cases as discussed in the text. The β of the heat-bath is considered to be 0.011×10^{18} nats.

$$\begin{aligned}
\lim_{\tau \rightarrow \infty} \tilde{S} &= \mathbf{S} \lim_{\tau \rightarrow \infty} \tilde{S}_D \mathbf{S}^{-1} \\
&= -2k \operatorname{Tr} \left[\mathbf{S} \left(\lim_{\tau \rightarrow \infty} \exp(\mathcal{D}) \right) \mathbf{S}^{-1} \mathbf{S} \left(\lim_{\tau \rightarrow \infty} \mathcal{D} \right) \mathbf{S}^{-1} \mathbf{S} \left(\lim_{\tau \rightarrow \infty} \exp(\mathcal{D}) \right) \mathbf{S}^{-1} \right], \quad (20) \\
&= -\frac{1}{2} \operatorname{Tr} [\rho_{SEA,0} \ln(\rho_{SEA,0})]
\end{aligned}$$

As we can see, the entropy functional reaches the quantum mechanical form as τ becomes large. We are now able to put in the conditions for micro-canonical or canonical $\rho_{SEA,0}$ as given in equations (7), and (8) in the limiting forms.

$$\begin{aligned}
\tilde{S}_{00} &= \\
&= -k^2 \operatorname{Tr} \left[\frac{\mathbf{I}_N}{\operatorname{Tr}\{\mathbf{I}_N\}^{1/e}} \mathbf{S} \exp \left(\frac{1-e}{ke} (\beta_H \mathbf{S}^{-1} \mathbf{H} \mathbf{S} + \beta_I) \right) \mathbf{S}^{-1} \times \frac{1-e}{ke} (\beta_H \mathbf{H} + \beta_I) \right]. \quad (21)
\end{aligned}$$

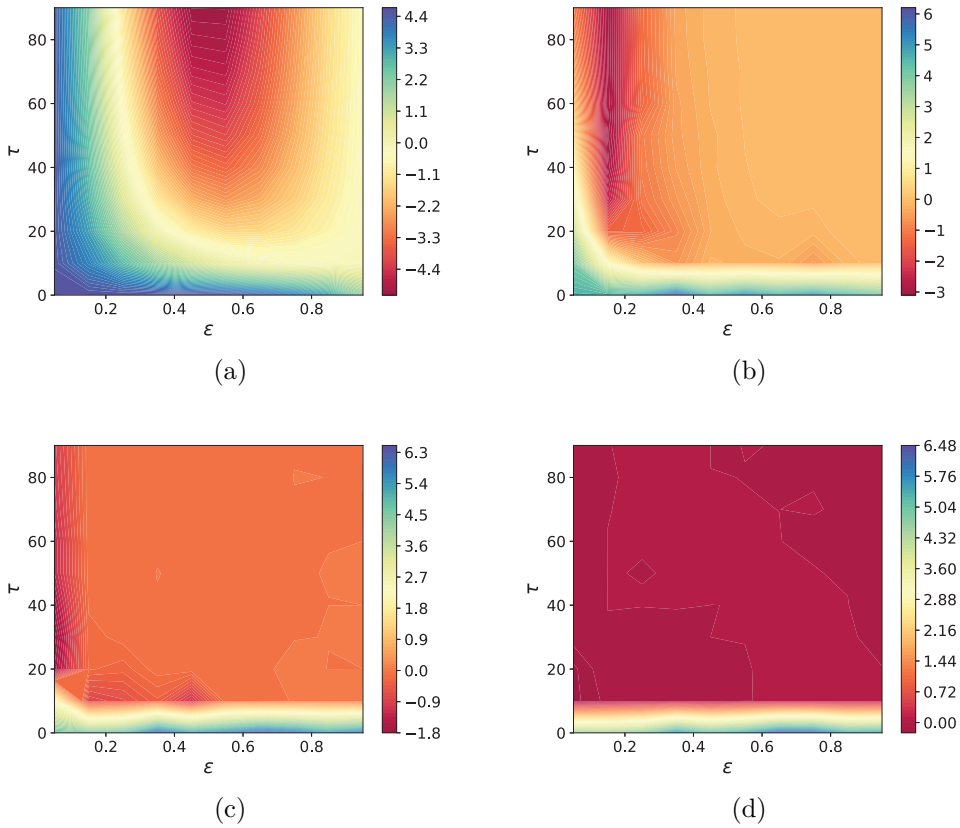


Figure 7. (Colour online) (a) to (d): $\tilde{S}(\gamma)$ distribution over different τ and ϵ values in time steps 1 to 4 respectively. The colour-bars accompanying each plot provide the range and contrast of the values in them. As time progresses the zero entropic zones almost engulf the available space in the panels.

And also,

$$\tilde{S}_{\infty 0} = 0 = \tilde{S}_{\infty 1} \quad (22)$$

At first in the case of single particles, we see a similar behaviour appear in the panels of Fig. 7. The panels confirm what we saw analytically in equations (21) and (22), and in Fig. 2 and 4. Higher τ begets unitary behaviour, and lower values of τ promotes higher entropy values.

For the case of the double particle walker, we have different behaviour in the growth of entropy which is dependent on the interaction between the systems. Systems with non-interacting or fermionic behaviour appear to have similar growth in their entropy values. And also, as was apparent from our analytic limits, the lower value of ϵ also ensures fastest entropy saturation in the form of blue line in Fig. 8. The distinction between the growths are not much which is to be expected as high temperature behaviour and micro-canonical behaviour appear to be identical. We have plotted similar plots for $\beta = 0.011 \times 10^{18}$ nats in the Fig. 9. Here we notice the similarities between non-interacting and fermionic entropy growth appears despite having different probability distributions (Fig.6). We also notice another behaviour absent hitherto, that is the

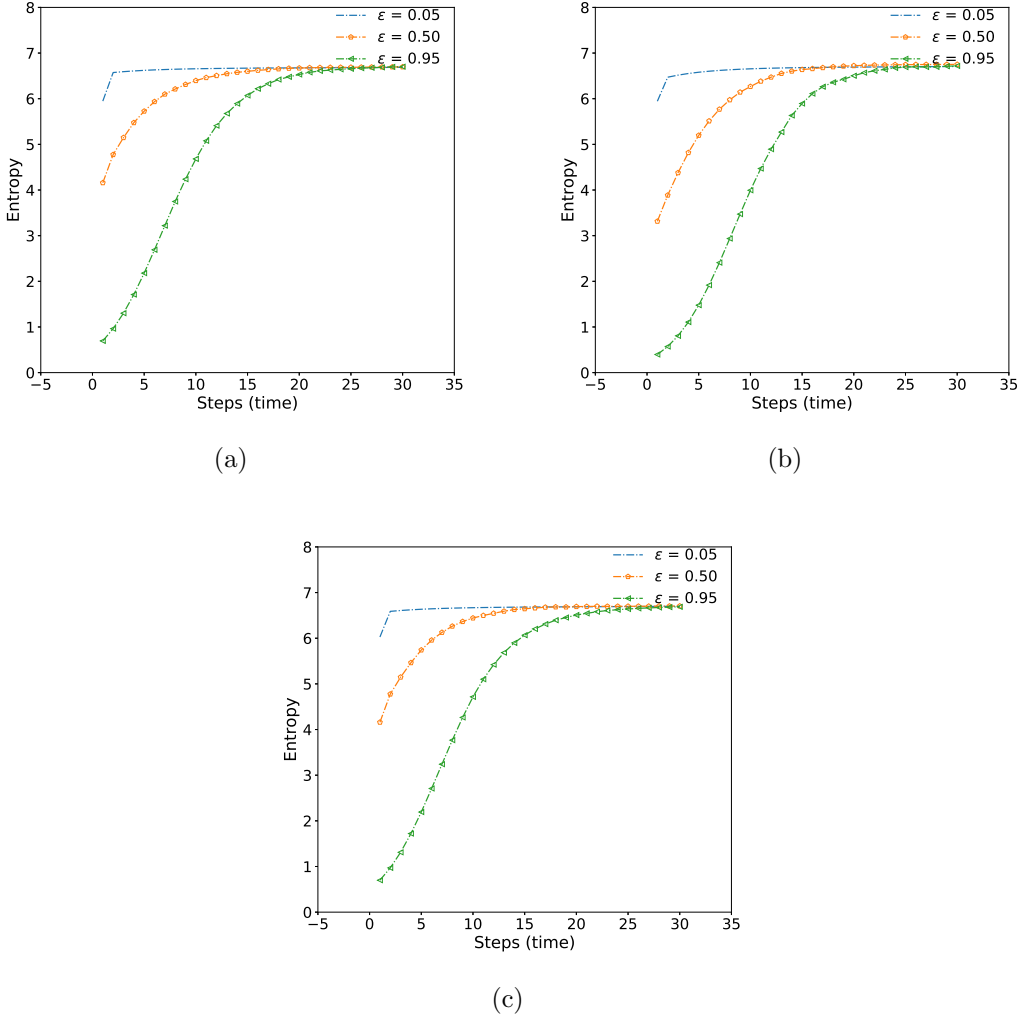


Figure 8. (Colour online) Entropy vs time (steps) for a double particle quantum walk on a ring of 30 nodes under SEA conditions, initiated at node 15, after 30 steps. The relaxation time τ is taken to be 90.02 (in (a) to (c)). ϵ is the dimensionless parameter denoting the perturbation of the initial state. Panels (a) for the non-interacting case, (b) for bosonic case, and the last one for the fermionic case.

difference between growth of entropy for $\epsilon = 0.5$ and the rest of the values. Suggesting further explorable avenues. The reason of such distinction between the two different type of evolutions as seen in Fig. 8 and 9 eludes our current scope, despite desiring a justification.

Using equation (A.6), we can write the rate of change of entropy functional (Π_S) using ρ from above (equation (15)) as follows (see, Appendix Appendix D, equation (D.3)).

$$\Pi_S = 2k \text{Tr} \left[\hat{L} \mathbf{S} \mathbf{D} \mathbf{S}^{-1} \mathbf{S} \mathbf{A}_0 \mathbf{S}^{-1} \exp \left(\exp \left(-4k \hat{L} t \right) - 1 \right) \mathbf{S} \exp \left(\mathcal{D} \right) \mathbf{S}^{-1} \right]. \quad (23)$$

As the above equation becomes too complex to treat analytically, we can still seek

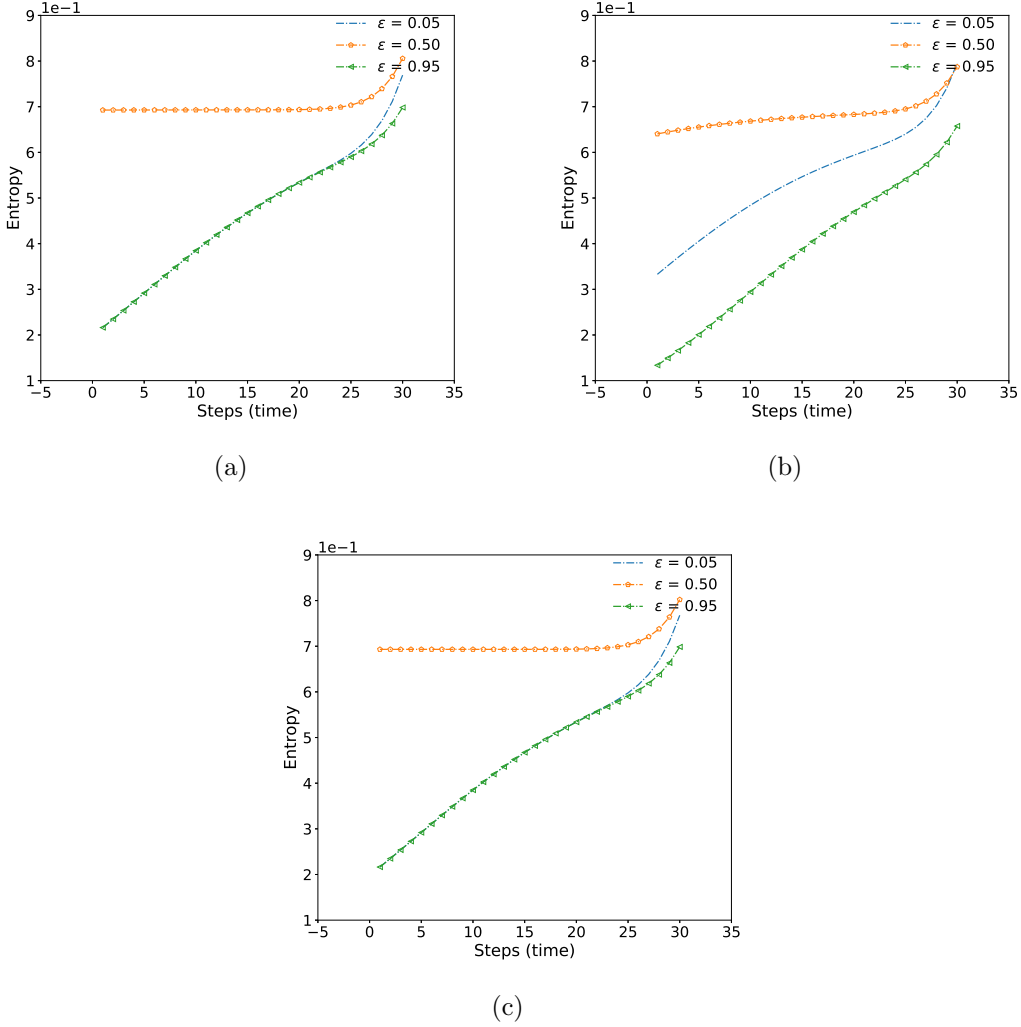


Figure 9. (Colour online) Entropy vs time (steps) for a double particle quantum walk on a ring of 30 nodes under SEA conditions, initiated at node 15, after 30 steps. The relaxation time τ is taken to be 90.02 (in (a) to (c)). ϵ is the dimensionless parameter denoting the perturbation of the initial state. The terms $1e-1$ appearing on the top left corner of the plots denote the order of magnitude of entropy values, which in this case is 10^{-1} . Panels (a) for the non-interacting case, (b) for bosonic case, and the last one for the fermionic case. The β of the heat-bath is considered to be 0.011×10^{18} nats.

out the limits of $\tau \rightarrow 0$ and some large limit $\tau \rightarrow \infty$.

$$\begin{aligned}
 & \Pi_S|_{\tau \rightarrow 0} \\
 &= \frac{1}{e} \text{Tr} \left[(k^2 \ln(\rho_{\text{SEA},0})^2 + k(2-e)(\beta_H \mathbf{H} + \beta_I) \ln(\rho_{\text{SEA},0}) + (1-e)(\beta_H \mathbf{H} + \beta_I)^2) (\rho_{\text{SEA},0})^{1/2e} \right. \\
 & \left. \mathbf{S} \exp \left(\frac{1-e}{2ke} (\beta_H \mathbf{S}^{-1} \mathbf{H} \mathbf{S} + \beta_I) \right) \mathbf{S}^{-1} \lim_{\tau \rightarrow 0} (\hat{L}) \right].
 \end{aligned} \tag{24}$$

In the right hand side of the equation (24), we see the presence of initial state ($\rho_{\text{SEA},0}$) in the limiting form, which may allow us in the future to go to the two extremes of ϵ limit and study the possible bifurcations present in this context. Similarly, taking the large limit of τ , we arrive at the following set of equations, *i.e.*, equations (25).

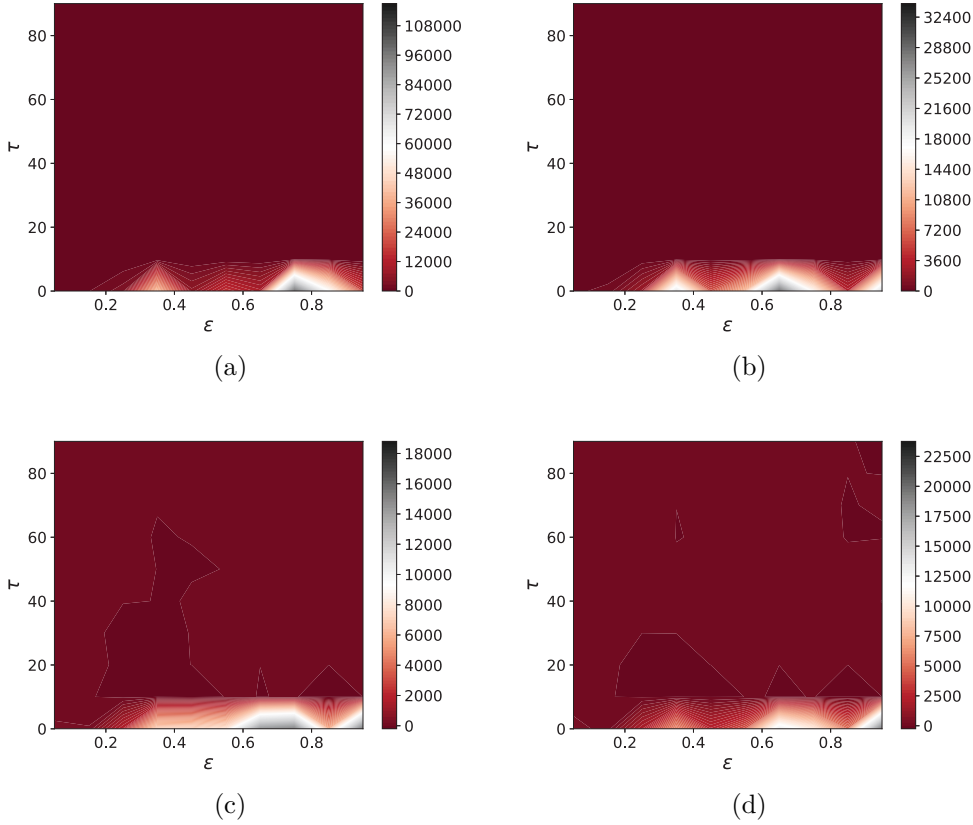


Figure 10. (Colour online) (a) to (d): Π_S distribution over different τ and ϵ values in time steps 1 to 4 respectively for a single walker. The colour-bars accompanying each plot provide the range and contrast of the values in them. In these panels, a rapid and sharp decrease in the rate of change of entropy functional can be observed across the panel. Also, the high valued zones are concentrated around certain set of (ϵ, τ) values.

Looking at equation (D.5), we see that for $\lim_{\tau \rightarrow 0} \mathcal{D}$ case all the terms in the above equation (equation (24)) are positive and the limit on \hat{L} drives the value of Π_S towards higher positive value. On the other hand, taking the limit for a large value of τ (in this case, infinity, numerically 90 is a sufficiently large value (see figure (2(a)))), results in the dip in \hat{L} contribution and the overall value of Π_S falls towards zero, albeit remaining positive (see equation D.7). The higher limits of τ can be written in the following way (see the derivation in equation (D.9)):

$$\Pi_S|_{\tau \rightarrow \infty} = k \text{Tr} \left[(k \ln(\rho_{\text{SEA},0})^2 + (\beta_H \mathbf{H} + \beta_I) \ln(\rho_{\text{SEA},0})) (\rho_{\text{SEA},0})^{1/2} \lim_{\tau \rightarrow \infty} (\hat{L}) \right]. \quad (25)$$

The only terms in equations (24,25) that are dependent on ϵ are the terms involving $\rho_{\text{SEA},0}$. Denoting $\lim_{\epsilon \rightarrow 0} \Pi_S|_{\tau \rightarrow 0}$ as $\Pi_{S,00}$ and $\lim_{\epsilon \rightarrow 1} \Pi_S|_{\tau \rightarrow 0}$ as $\Pi_{S,01}$ and using the similar format we find:

$$\Pi_{S,00} = \frac{1}{e} \text{Tr} \left[(1-e)(\beta_H \mathbf{H} + \beta_I)^2 \frac{\mathbf{I}_N}{\text{Tr}\{\mathbf{I}_N\}^{1/2e}} \mathbf{S} \exp \left(\frac{1-e}{2ke} (\beta_H \mathbf{S}^{-1} \mathbf{H} \mathbf{S} + \beta_I) \right) \mathbf{S}^{-1} \lim_{\tau \rightarrow 0} (\hat{L}) \right] \quad (26)$$

And, the $\lim_{\epsilon \rightarrow 0} \Pi_S|_{\tau \rightarrow \infty}$ term, or $\Pi_{S,\infty 0}$ is found to be:

$$\Pi_{S,\infty 0} = 0 \quad (27)$$

Evidently, for low values of τ , we can safely say that the limits tend to blow up because of the involvement of $\lim_{\tau \rightarrow 0} (\hat{L})$. Which is not surprising, and thus a lower estimate on τ still remains a mystery to us. On the other hand, if we look at the equation (27), we see that despite the entropy production rate being positive, it reaches a zero value.

When looked across the panels in figure (10), we see that the contours denoting the peaks of high rate of change of entropy, Π_S (shaded in black) are largely confined to the low τ values only. It is also to be noted that there is a sharp rise in values near $\tau = 1$, rest of the portions ($\tau > 1$) in all the panels have a zero valued flatland, owing to constant entropy (i.e., unitary evolution) region. This has two implications, firstly as thermal states are indistinguishable from the background, low τ states become obsolete from experimentation point of view. The region of thermalization also being spread over the entirety of range available to τ , we find it difficult to identify any specific trait of evolution to estimate the value of τ for the given system as discussed by [25].

4. Conclusion

In this paper, we had set out to solve the continuous time quantum walker (CTQW) for both single and double particle case under the assumptions enforced by the steepest entropy ascent (SEA) ansatz. We have solved the CTQW on a regular ring graph of 100 and 30 nodes for single and double walker respectively. In both the cases we have considered micro-canonical and canonical scenarios. In the case of double walker, we have considered non-interacting and also interacting walkers. We have evolved the states using the iterative solution presented in the paper. We have plotted the probability distributions under various limits and have found some interesting results. We have noticed the presence of typical canonical distribution and unitary probability distribution which depend on the amount of perturbation and relaxation time of the system. We also have plotted the growth of entropy functional as step size is increased and we are provided with intriguing growth patterns. That SEA can govern a motion which under different limits turn into either typical or MBL phases. This connection has the potential to act as a coherent set of theories with SEA explaining away the mechanism and ETH/MBL exploring the emergent phenomena. This requires further

investigation. Our results indicate certain dependencies on initial conditions which do not rule away the role of chaos in the evolution into the thermal behaviour. This claim needs to be investigated further. We have solved the QW for hypercube graph as well only to find similar behaviours. Our results suggest further exploration into the evolution of entropy under SEA, and we intend to follow that up.

5. Acknowledgment

The author would take this opportunity to thank his guide and mentor Prof. Sonjoy Majumder for his inspiration. The author would also extend his gratitude for the esteemed reviewers for their encouraging comments. He would like to thank the Department of Science and Technology, Government of India, for funding his research under the INSPIRE Fellowship scheme.

Appendix A.

If the states are functions of time (t) only, $\gamma = \gamma(t)$, their time evolution obeys the equation of motion,

$$\left| \frac{d\gamma}{dt} \right\rangle = |\Pi_\gamma\rangle, \quad (\text{A.1})$$

where $|\Pi_\gamma\rangle$ is also an element of \mathcal{L} such that the rates of change of the entropy $\tilde{S}(\gamma)$ and of any other conserved property $\tilde{C}_i(\gamma)$, with i labelling a list of conserved properties, are

$$\frac{dS}{dt} = \Pi_S \quad \text{with} \quad \Pi_S = (\Phi | \Pi_\gamma) \geq 0, \quad (\text{A.2})$$

$$\frac{dC_i}{dt} = \Pi_{C_i} \quad \text{with} \quad \Pi_{C_i} = (\Psi_i | \Pi_\gamma) = 0, \quad (\text{A.3})$$

where Π_S and Π_{C_i} are the respective production rates and $|\Phi\rangle = \left| \delta\tilde{S}(\gamma)/\delta\gamma \right\rangle$. $|\Psi_i\rangle = \left| \delta\tilde{C}_i(\gamma)/\delta\gamma \right\rangle$ are shorthand notations for denoting the variational derivatives with respect to γ of the entropy functional $\tilde{S}(\gamma)$ and the conserved functionals $\tilde{C}_i(\gamma)$, respectively. The set of operators which correspond to the conserved quantities can be written as follows:

$$\{C_i\} = \{H, M_x, M_y, M_z, N_1, N_2, \dots, N_r, I\}. \quad (\text{A.4})$$

It is assumed that these are self-adjoint operators in \mathcal{L} , and each of M_i, N_j commutes with H . The equations for Π_{C_i} turn out to be of the following form:

$$\Pi_{C_i} = (2C_i\gamma | \Pi_\gamma) = 0. \quad (\text{A.5})$$

The entropy functional turns out to be,

$$\Pi_S = -k \frac{d}{dt} \text{Tr}(\rho \ln(\rho)) = (-2k(\ln(\gamma\gamma^\dagger)) | \Pi_\gamma). \quad (\text{A.6})$$

In absence of any driving agents, Π_γ is tangent to the path $\gamma(t)$, letting us to consider a suitable metric $\hat{G}(\gamma)$ associated with \mathcal{L} so that we can measure the length element in the state space. The metric is a real, symmetric and positive semi-definite operator on the state space, and is used as follows [see [59, 25]]:

$$dl = \sqrt{(\Pi_\gamma | \hat{G}(\gamma) | \Pi_\gamma)} dt. \quad (\text{A.7})$$

Using variational approach, one can find the Lagrangian associated with SEA principle as follows [25],

$$\Upsilon = \Pi_S - \sum_i \beta_i \Pi_{C_i} - \frac{\tau}{2} (\Pi_\gamma | \hat{G}(\gamma) | \Pi_\gamma), \quad (\text{A.8})$$

β_i and $\tau/2$ are Lagrange multipliers independent of Π_γ . The above equation can be reshaped using equations (A.2) and (A.3) and then on taking the functional derivative of Υ with respect to $|\Pi_\gamma\rangle$ we get,

$$\frac{\delta \Upsilon}{\delta \Pi_\gamma} = |\Phi\rangle - \sum_i \beta_i |\Psi_i\rangle - \tau \hat{G}(\gamma) |\Pi_\gamma\rangle. \quad (\text{A.9})$$

And the equation of motion is found setting $\frac{\delta \Upsilon}{\delta \Pi_\gamma} = 0$,

$$|\Pi_\gamma\rangle = \hat{L} \left| \Phi - \sum_i \beta_i \Psi_i \right\rangle, \quad (\text{A.10})$$

where

$$\hat{L} = \frac{1}{\tau} \hat{G}(\gamma)^{-1}. \quad (\text{A.11})$$

From equation (2) we can write,

$$\frac{d\rho}{dt} = \frac{d\gamma}{dt} \gamma^\dagger + \gamma \frac{d\gamma^\dagger}{dt}. \quad (\text{A.12})$$

For our case, we are interested in the conserved quantities \mathbf{H} and \mathbf{I} . hence, using equation (A.10), we get,

$$\frac{d\rho}{dt} = -2\hat{L} [k[\ln(\rho), \rho]_+ + \beta_H [\mathbf{H}, \rho]_+ + \beta_I [\mathbf{I}, \rho]_+] - \frac{i}{\hbar} [\mathbf{H}, \rho]_-. \quad (\text{A.13})$$

Appendix B.

Using the constraints of equations (A.2-A.3) we get,

$$\sum_i (\gamma \mathbf{H} | \hat{L} | \Psi_i) \beta_i = -2k (\gamma \mathbf{H} | \hat{L} | \ln(\gamma \gamma^\dagger) \gamma). \quad (\text{B.1})$$

This equation can be solved using Cramer's rule for solving linear equation with multiple variables, provided the solution exists, which is equivalent to the following expression:

$$\det(\Delta) = \det \begin{bmatrix} -(\gamma \mathbf{H} | \hat{L} | \mathbf{H} \gamma) & (\gamma \mathbf{H} | \hat{L} | \gamma) \\ -(\gamma | \hat{L} | \mathbf{H} \gamma) & (\gamma | \hat{L} | \gamma) \end{bmatrix} \neq 0. \quad (\text{B.2})$$

Knowing these, we can straight away compute the β_i 's as follows:

$$\beta_H = \frac{1}{\det(\Delta)} \begin{vmatrix} -k(\gamma \mathbf{H} | \hat{L} | \ln(\gamma \gamma^\dagger) \gamma) & (\gamma \mathbf{H} | \hat{L} | \gamma) \\ k(\gamma | \hat{L} | \ln(\gamma \gamma^\dagger) \gamma) & (\gamma | \hat{L} | \gamma) \end{vmatrix}, \quad (\text{B.3})$$

$$\beta_I = \frac{1}{\det(\Delta)} \begin{vmatrix} -(\gamma \mathbf{H} | \hat{L} | \mathbf{H} \gamma) & -k(\gamma \mathbf{H} | \hat{L} | \ln(\gamma \gamma^\dagger) \gamma) \\ -(\gamma | \hat{L} | \mathbf{H} \gamma) & k(\gamma | \hat{L} | \ln(\gamma \gamma^\dagger) \gamma) \end{vmatrix}. \quad (\text{B.4})$$

Looking at the expressions of β_i 's we can say that they don't have an explicit dependence on τ . As \hat{L} is essentially $1/\tau$ multiplied to the inverse of the identity operator (the metric that we chose), and it appears in both the numerator and the denominator of the expressions.

Appendix C.

We use diagonalization method to have a guess at the solution. First, the similarity transformation \blacklozenge of $\gamma = \mathbf{S} \gamma_D \mathbf{S}^{-1}$ (where γ_D is the diagonal matrix) across both sides of the equation (14) allows us to write it down in the following form

$$\frac{d\gamma_D}{dt} = \Pi_{\gamma_D} = \hat{L} \left[-2k \ln(\gamma_D \gamma_D^\dagger) \gamma_D - 2\beta_H \mathbf{S}^{-1} \mathbf{H} \mathbf{S} \gamma_D - 2\beta_I \gamma_D \right]. \quad (\text{C.1})$$

In this form, it is easier to guess the trial solution to be of the form,

$$\gamma_D = e^{\mathcal{D}(t)}, \quad (\text{C.2})$$

Equation (C.1) on substitution using equation (C.2) yields,

$$\gamma_D = \exp \left(\frac{A_0 \exp(\exp(-4k\hat{L}t) - 1) - \beta_H \mathbf{S}^{-1} \mathbf{H} \mathbf{S} - \beta_I}{2k} \right), \quad (\text{C.3})$$

where,

$$\mathcal{D}(t) = \frac{A_0 \exp(\exp(-4k\hat{L}t) - 1) - \beta_H \mathbf{S}^{-1} \mathbf{H} \mathbf{S} - \beta_I}{2k},$$

and, A_0 is given by

$$A_0 = k \ln(\gamma_{D,0} \gamma_{D,0}^\dagger) + \beta_H \mathbf{S}^{-1} \mathbf{H} \mathbf{S} + \beta_I \quad (\text{C.4})$$

thus allowing us to write the SEA evolution as (referring to equation (2)),

$$\rho_{\text{SEA},t} = e^{-i\mathbf{H}t} \mathbf{S} e^{\mathcal{D}(t)} (e^{\mathcal{D}(t)})^\dagger \mathbf{S}^{-1} e^{i\mathbf{H}t} \quad (\text{C.5})$$

Here we have obtained a solution which for each time step of the process of evaluating $\rho_{\text{SEA},t}$ is iterative in nature. We have avoided integrating because of the involvement of

\blacklozenge Since the square root is taken to be positive, every γ can be diagonalized.

the factor τ . Its appearance in the exponent in the evolution of γ_D allows us to increase or decrease the time slice under which we are considering the SEA evolution. Thus, it acts as a time-step, or resolution for lack of a better word. Besides, the value of τ may not remain constant, although making it so doesn't affect the physics (see, [25]). When interpreted this way, we find surprising effects on the overall dynamics. When taken total time derivative of equation (C.5), and a little bit of rearrangement, we end up recovering equation (A.13).

Appendix D.

Using equation (A.6) and equation (C.1), we can write,

$$\Pi_{S_D} = -2k \left(\ln \left(\gamma_D \gamma_D^\dagger \right) \mid \Pi_{\gamma_D} \right). \quad (\text{D.1})$$

This allows us to use equation (C.3), and the fact $\mathcal{D}(t) = \mathcal{D}^\dagger(t)$, and compute Π_{S_D} as follows:

$$\begin{aligned} \Pi_{S_D} &= 2k \text{Tr} \left[\hat{L} \left[(2\mathcal{D} \mid 4k\mathcal{D} \exp(\mathcal{D})) \right. \right. \\ &\quad \left. \left. + (2\mathcal{D} \mid 2\beta_H \mathbf{S}^{-1} \mathbf{H} \mathbf{S} \exp(\mathcal{D})) + (2\mathcal{D} \mid 2\beta_I \exp(\mathcal{D})) \right] \right], \quad (\text{D.2}) \\ &= 2k \text{Tr} \left[\hat{L} \mathcal{D} \left[2k\mathcal{D} + \beta_H \mathbf{S}^{-1} \mathbf{H} \mathbf{S} + \beta_I \right] \exp(\mathcal{D}) \right]. \end{aligned}$$

Which on simplification gives (using the expression for \mathcal{D} as given in Appendix C),

$$\begin{aligned} \Pi_{S_D} &= 2k \text{Tr} \left[\hat{L} \mathcal{D} A_0 \exp \left(\exp \left(-4k\hat{L}t \right) - 1 \right) \right. \\ &\quad \left. \times \exp(\mathcal{D}) \right], \\ \implies \Pi_S &= \mathcal{S} \Pi_{S_D} \mathbf{S}^{-1} \quad (\text{D.3}) \\ &= 2k \text{Tr} \left[\hat{L} \mathcal{S} \mathcal{D} \mathbf{S}^{-1} \mathbf{S} A_0 \mathbf{S}^{-1} \exp \left(\exp \left(-4k\hat{L}t \right) - 1 \right) \right. \\ &\quad \left. \times \mathbf{S} \exp(\mathcal{D}) \mathbf{S}^{-1} \right], \end{aligned}$$

For the purpose of computation, we calculate $\lim_{\tau \rightarrow 0} \mathcal{D}$ as follows:

$$\begin{aligned} \lim_{\tau \rightarrow 0} \mathcal{D} &= \\ &= \lim_{\tau \rightarrow 0} \left(\frac{A_0 \exp \left(\exp \left(-4k\hat{L}t \right) - 1 \right) - \beta_H \mathbf{S}^{-1} \mathbf{H} \mathbf{S} - \beta_I}{2k} \right), \quad (\text{D.4}) \\ &= \frac{A_0}{2ke} - \frac{\beta_H \mathbf{S}^{-1} \mathbf{H} \mathbf{S}}{2k} - \frac{\beta_I}{2k}, \\ &= \frac{\ln \left(\gamma_{D,0} \gamma_{D,0}^\dagger \right)}{2e} + \frac{1-e}{2ke} \left(\beta_H \mathbf{S}^{-1} \mathbf{H} \mathbf{S} + \beta_I \right). \end{aligned}$$

Applying similarity transformation on this, we get:

$$\mathbf{S} \left(\lim_{\tau \rightarrow 0} \mathcal{D} \right) \mathbf{S}^{-1} = \frac{\ln(\rho_{\text{SEA},0})}{2e} + \frac{1-e}{2ke} (\beta_H \mathbf{H} + \beta_I). \quad (\text{D.5})$$

And we also have,

$$\begin{aligned} \lim_{\tau \rightarrow \infty} \mathcal{D} &= \\ & \lim_{\tau \rightarrow \infty} \left(\frac{A_0 \exp\left(\exp(-4k\hat{L}t) - 1\right) - \beta_H \mathbf{S}^{-1} \mathbf{H} \mathbf{S} - \beta_I}{2k} \right), \\ &= \frac{A_0}{2k} - \frac{\beta_H \mathbf{S}^{-1} \mathbf{H} \mathbf{S}}{2k} - \frac{\beta_I}{2k}, \\ &= \frac{\ln(\gamma_{D,0} \gamma_{D,0}^\dagger)}{2}. \end{aligned} \quad (\text{D.6})$$

Leading us to,

$$\mathbf{S} \left(\lim_{\tau \rightarrow \infty} \mathcal{D} \right) \mathbf{S}^{-1} = \frac{\ln(\rho_{\text{SEA},0})}{2}. \quad (\text{D.7})$$

Now, we can compute the limits as follow:

$$\begin{aligned} & \Pi_S|_{\tau \rightarrow 0} \\ &= 2k \text{Tr} \left[\lim_{\tau \rightarrow 0} \left(\hat{L} \mathbf{S} \mathcal{D} \mathbf{S}^{-1} \mathbf{S} A_0 \mathbf{S}^{-1} \right. \right. \\ & \quad \left. \left. \times \exp\left(\exp(-4k\hat{L}t) - 1\right) \mathbf{S} \exp(\mathcal{D}) \mathbf{S}^{-1} \right) \right], \\ &= 2k \text{Tr} \left[\lim_{\tau \rightarrow 0} (\hat{L}) \left(\mathbf{S} \left(\lim_{\tau \rightarrow 0} \mathcal{D} \right) \mathbf{S}^{-1} \right) \frac{\mathbf{S} A_0 \mathbf{S}^{-1}}{e} \right. \\ & \quad \left. \times \mathbf{S} \lim_{\tau \rightarrow 0} \exp(\mathcal{D}) \mathbf{S}^{-1} \right], \\ &= 2k \text{Tr} \left[\lim_{\tau \rightarrow 0} (\hat{L}) \left(\frac{\ln(\rho_{\text{SEA},0})}{2e} + \frac{1-e}{2ke} (\beta_H \mathbf{H} + \beta_I) \right) \right. \\ & \quad \left. \times \frac{k \ln(\rho_{\text{SEA},0}) + \beta_H \mathbf{H} + \beta_I}{e} \mathbf{S} \lim_{\tau \rightarrow 0} \exp(\mathcal{D}) \mathbf{S}^{-1} \right] \\ & \Pi_S|_{\tau \rightarrow 0} = \\ & \frac{1}{e} \text{Tr} \left[(k^2 \ln(\rho_{\text{SEA},0})^2 + k(2-e)(\beta_H \mathbf{H} + \beta_I) \ln(\rho_{\text{SEA},0}) \right. \\ & \quad \left. + (1-e)(\beta_H \mathbf{H} + \beta_I)^2) \lim_{\tau \rightarrow 0} (\hat{L}) \right. \\ & \quad \left. \times \mathbf{S} \exp\left(\frac{\ln(\rho_{\text{SEA},0})}{2e} + \frac{1-e}{2ke} (\beta_H \mathbf{S}^{-1} \mathbf{H} \mathbf{S} + \beta_I)\right) \mathbf{S}^{-1} \right], \\ &= \frac{1}{e} \text{Tr} \left[(k^2 \ln(\rho_{\text{SEA},0})^2 + k(2-e)(\beta_H \mathbf{H} + \beta_I) \ln(\rho_{\text{SEA},0}) \right. \\ & \quad \left. + (1-e)(\beta_H \mathbf{H} + \beta_I)^2) (\rho_{\text{SEA},0})^{1/2e} \right. \\ & \quad \left. \times \mathbf{S} \exp\left(\frac{1-e}{2ke} (\beta_H \mathbf{S}^{-1} \mathbf{H} \mathbf{S} + \beta_I)\right) \mathbf{S}^{-1} \lim_{\tau \rightarrow 0} (\hat{L}) \right]. \end{aligned} \quad (\text{D.8})$$

And the other limit can be similarly calculated as follows:

$$\begin{aligned}
\Pi_S|_{\tau \rightarrow \infty} &= \\
& 2k \operatorname{Tr} \left[\lim_{\tau \rightarrow \infty} \left(\hat{L} \mathbf{S} \mathcal{D} \mathbf{S}^{-1} \mathbf{S} A_0 \mathbf{S}^{-1} \right. \right. \\
& \quad \left. \left. \times \exp \left(\exp \left(-4k \hat{L} t \right) - 1 \right) \mathbf{S} \exp(\mathcal{D}) \mathbf{S}^{-1} \right) \right] \\
&= 2k \operatorname{Tr} \left[\lim_{\tau \rightarrow \infty} (\hat{L}) \left(\mathbf{S} \left(\lim_{\tau \rightarrow \infty} \mathcal{D} \right) \mathbf{S}^{-1} \right) \mathbf{S} A_0 \mathbf{S}^{-1} \right. \\
& \quad \left. \times \mathbf{S} \lim_{\tau \rightarrow \infty} \exp(\mathcal{D}) \mathbf{S}^{-1} \right], \\
&= 2k \operatorname{Tr} \left[\lim_{\tau \rightarrow \infty} (\hat{L}) \left(\frac{\ln(\rho_{\text{SEA},0})}{2} \right) \right. \\
& \quad \left. \times (k \ln(\rho_{\text{SEA},0}) + \beta_H \mathbf{H} + \beta_I) \mathbf{S} \lim_{\tau \rightarrow \infty} \exp(\mathcal{D}) \mathbf{S}^{-1} \right], \tag{D.9} \\
&= k \operatorname{Tr} \left[(k \ln(\rho_{\text{SEA},0})^2 + (\beta_H \mathbf{H} + \beta_I) \ln(\rho_{\text{SEA},0})) \right. \\
& \quad \left. \times \lim_{\tau \rightarrow \infty} (\hat{L}) \exp \left(\frac{\ln(\rho_{\text{SEA},0})}{2} \right) \right], \\
&= k \operatorname{Tr} \left[(k \ln(\rho_{\text{SEA},0})^2 + (\beta_H \mathbf{H} + \beta_I) \ln(\rho_{\text{SEA},0})) \right. \\
& \quad \left. (\rho_{\text{SEA},0})^{1/2} \lim_{\tau \rightarrow \infty} (\hat{L}) \right].
\end{aligned}$$

- [1] Breuer H P, Petruccione F *et al.* 2002 *The theory of open quantum systems* (Oxford University Press on Demand)
- [2] Tasaki H 1998 *Phys. Rev. Lett.* **80**(7) 1373–1376
- [3] Popescu S, Short A J and Winter A 2006 *Nature Physics* **2** 754 EP – article
- [4] Goldstein S, Lebowitz J L, Tumulka R and Zanghì N 2006 *Phys. Rev. Lett.* **96**(5) 050403
- [5] Garnerone S, de Oliveira T R and Zanardi P 2010 *Phys. Rev. A* **81**(3) 032336
- [6] Santos L F, Polkovnikov A and Rigol M 2012 *Phys. Rev. E* **86**(1) 010102
- [7] Gring M, Kuhnert M, Langen T, Kitagawa T, Rauer B, Schreitl M, Mazets I, Smith D A, Demler E and Schmiedmayer J 2012 *Science* 0036-8075
- [8] Eisert J, Friesdorf M and Gogolin C 2015 *Nature Physics* **11** 124 EP – review Article
- [9] Reimann P 2016 *Nature Communications* **7** 10821 EP – article
- [10] Tasaki H 2016 *Journal of Statistical Physics* **163** 937–997 1572-9613
- [11] Abanin D A and Papi Z *Annalen der Physik* **529** 1700169
- [12] Alba V and Calabrese P 2017 *Proceedings of the National Academy of Sciences* **114** 7947–7951 0027-8424
- [13] Rauer B, Erne S, Schweigler T, Cataldini F, Tajik M and Schmiedmayer J 2018 *Science* 0036-8075
- [14] Anza F 2018 *Entropy* **20** 1099-4300
- [15] Ashida Y, Saito K and Ueda M 2018 *Phys. Rev. Lett.* **121**(17) 170402
- [16] Vosk R, Huse D A and Altman E 2015 *Physical Review X* **5** 031032
- [17] Potter A C, Vasseur R and Parameswaran S 2015 *Physical Review X* **5** 031033
- [18] Luitz D J, Huveneers F and De Roeck W 2017 *Physical review letters* **119** 150602
- [19] Hatsopoulos G N and Gyftopoulos E P 1976 *Foundations of Physics* **6** 15–31 1572-9516
- [20] Hatsopoulos G N and Gyftopoulos E P 1976 *Foundations of Physics* **6** 127–141 1572-9516
- [21] Hatsopoulos G N and Gyftopoulos E P 1976 *Foundations of Physics* **6** 439–455 1572-9516
- [22] Hatsopoulos G N and Gyftopoulos E P 1976 *Foundations of Physics* **6** 561–570 1572-9516
- [23] Beretta G P, Gyftopoulos E P, Park J L and Hatsopoulos G N 1984 *Il Nuovo Cimento B (1971-1996)* **82** 169–191 1826-9877

- [24] Beretta G P, Gyftopoulos E P and Park J L 1985 *Il Nuovo Cimento B (1971-1996)* **87** 77–97 1826-9877
- [25] Beretta G P 2014 *Physical Review E* **90** 042113
- [26] Gheorghiu-Svirschevski S 2001 *Phys. Rev. A* **63**(2) 022105
- [27] Beretta G P 2010 *Journal of Physics: Conference Series* **237** 012004
- [28] Beretta G P 1987 Steepest entropy ascent in quantum thermodynamics *The Physics of Phase Space Nonlinear Dynamics and Chaos Geometric Quantization, and Wigner Function* ed Kim Y S and Zachary W W (Berlin, Heidelberg: Springer Berlin Heidelberg) pp 441–443 978-3-540-47901-7
- [29] Cano-Andrade S, Beretta G P and von Spakovsky M R 2015 *Phys. Rev. A* **91** 013848
- [30] Li G, von Spakovsky M R and Hin C 2018 *Physical Review B* **97** 024308
- [31] Montefusco A, Consonni F and Beretta G P 2015 *Physical Review E* **91** 042138
- [32] Kim I and von Spakovsky M R 2017 *Phys. Rev. E* **96**(2) 022129
- [33] Childs A M and Goldstone J 2004 *Phys. Rev. A* **70**(2) 022314
- [34] Shenvi N, Kempe J and Whaley K B 2003 *Phys. Rev. A* **67**(5) 052307
- [35] Childs A M 2009 *Physical review letters* **102** 180501
- [36] Aharonov Y, Davidovich L and Zagury N 1993 *Phys. Rev. A* **48**(2) 1687–1690
- [37] Nayak A and Vishwanath A 2000 *arXiv preprint quant-ph/0010117*
- [38] Omar Y, Paunković N, Sheridan L and Bose S 2006 *Phys. Rev. A* **74**(4) 042304
- [39] Pathak P K and Agarwal G S 2007 *Phys. Rev. A* **75**(3) 032351
- [40] Rohde P P, Schreiber A, tefak M, Jex I and Silberhorn C 2011 *New Journal of Physics* **13** 013001
- [41] Rohde P P, Fedrizzi A and Ralph T C 2012 *Journal of Modern Optics* **59** 710–720
- [42] Duda J 2012 *Journal of Physics: Conference Series* **361** 012039
- [43] Brun T A, Carteret H A and Ambainis A 2003 *Physical Review A* **67** 052317
- [44] Romanelli A, Donangelo R, Portugal R and Marquezino F d L 2014 *Phys. Rev. A* **90**(2) 022329
- [45] Romanelli A 2012 *Phys. Rev. A* **85**(1) 012319
- [46] Du J, Li H, Xu X, Shi M, Wu J, Zhou X and Han R 2003 *Phys. Rev. A* **67**(4) 042316
- [47] Bromberg Y, Lahini Y, Morandotti R and Silberberg Y 2009 *Phys. Rev. Lett.* **102** 253904
- [48] Karski M, Förster L, Choi J M, Steffen A, Alt W, Meschede D and Widera A 2009 *Science* **325** 174–177 0036-8075
- [49] Gard B T, Cross R M, Anisimov P M, Lee H and Dowling J P 2013 *JOSA B* **30** 1538–1545
- [50] Manouchehri K and Wang J 2014 *Physical Implementation of Quantum Walks* (Berlin, Heidelberg: Springer Berlin Heidelberg) 978-3-642-36014-5
- [51] Farhi E and Gutmann S 1998 *Phys. Rev. A* **57**(4) 2403–2406
- [52] Rohde P P, Brennen G K and Gilchrist A 2013 *Phys. Rev. A* **87**(5) 052302
- [53] Cano-Andrade S, Beretta G P and von Spakovsky M R 2015 *Phys. Rev. A* **91**(1) 013848
- [54] Nielsen M A and Chuang I L 2000
- [55] BERETTA G P
- [56] BERETTA G P 2005 *Modern Physics Letters A* **20** 977–984
- [57] Farhi E and Gutmann S 1998 *Phys. Rev. A* **58**(2) 915–928
- [58] Yan L L, Xiong T P, Rehan K, Zhou F, Liang D F, Chen L, Zhang J Q, Yang W L, Ma Z H and Feng M 2018 *Phys. Rev. Lett.* **120**(21) 210601
- [59] Beretta G P 2009 *Reports on Mathematical Physics* **64** 139 – 168 0034-4877